Proximity-Induced Superconductivity in New Superstructures on 2H-$NbSe_2$ Surface *

Xing-Yuan Hou(侯兴元)[1,2], Ya-Dong Gu(谷亚东)[1,2], Zong Wang(王宗)[1,2], Hai Zi(子海)[2], Xiang-De Zhu(朱相德)[3**], Meng-Di Zhang (张孟迪)[1], Chun-Hong Li(李春红)[1], Cong Ren(任聪)[1], Lei Shan(单磊)[1,2,4**]

[1]*Beijing National Laboratory for Condensed Matter Physics, Institute of Physics, Chinese Academy of Sciences, Beijing 100190*

[2]*School of Physical Sciences, University of Chinese Academy of Sciences, Beijing 100049*

[3]*Anhui Province Key Laboratory of Condensed Matter Physics at Extreme Conditions, High Magnetic Field Laboratory of the Chinese Academy of Science, Hefei 230031*

[4]*Collaborative Innovation Center of Quantum Matter, Beijing 100190*

(Received 25 April 2017)

Using scanning tunneling microscopy we observe a stripe phase smoothly interfacing with a triangular 2×2 superstructure on the surface of 2H-$NbSe_2$ single crystal. Proximity-induced superconductivity is demonstrated in these new ordered structures by measurements of low-temperature tunneling spectra. The modulation of superconductivity by the reconstruction provides an opportunity to understand the interplay between superconductivity and charge orders.

PACS: 74.45.+c, 71.45.Lr, 74.50.+r, 74.78.Fk DOI: 10.1088/0256-307X/34/7/077403

Coexistence or competition between superconductivity and charge-ordered states has attracted tremendous interest in the field of condensed matter physics, which is closely related to the abnormal properties of some unconventional superconductors.[1–4] In addition to the materials containing both superconductivity and charge orders, the proximity effect is another choice to be used to study such coexistence/competition. When a normal metal with charge orders is placed in electrical contact with a superconductor, weak superconductivity may occur in the normal metal side via the 'leakage' of Cooper pairs, i.e., the proximity effect. As ideal platforms for this study, the quasi-two-dimensional transition metal dichalcogenides (TMDs) have diverse electronic states including charge density waves (CDWs),[5,6] electronic topology,[7–9] and intrinsic or doping induced superconductivity.[10] The weak van der Waals interaction between layers make TMDs easily downsized to a single or a few layers.[11–15] Furthermore, the surface structure of most TMDs is sensitive to defects, local strains and thermal perturbations, exampled by the transitions between different polymorphs in the cleaving process of 2H-MX_2.[16–22] It may provide a unique way to understand the interplay between superconductivity and charge orders.

Among TMDs, 2H-$NbSe_2$ has been studied intensively due to the coexistence of superconductivity and CDW below a relatively high critical temperature of $T_c \sim 7.1$ K after the emergence of an incommensurate 3×3 CDW at 33 K.[6,23] In this Letter, we report two new superstructures observed on the cleaved surface of 2H-$NbSe_2$ single crystal by using a low-temperature scanning tunneling microscope (STM). Distinct from the common 3×3 CDW, one of the new structures is a triangular 2×2 ($3Q$) phase, and the other one has a stripe configuration ($1Q$). These two phases interface smoothly with each other and their electronic density of states (DOS) are quite different from that of 2H-$NbSe_2$. Demonstration of proximity-induced superconductivity in these phases allows us to investigate the interplay of superconductivity and charge orders at a microscopic level.

The 2H-$NbSe_2$ single crystals were grown by the iodine vapor transport method.[24] A single crystalline sample was cold-cleaved *in situ* and then was inserted into the home-built low-temperature STM immediately. An electrochemically etched tungsten tip was used for the STM measurements after field emission treatment on a piece of Au. A constant current mode was adopted to obtain topographic images by applying a bias voltage to the sample. The tunneling spectra of differential conductance versus voltage were obtained using a standard lock-in technique.

Figure 1(a) shows an overview topographic image of the sample surface, containing both $1Q$ and $3Q$ phases. A profile taken along the arrowed line in Fig. 1(a) is given in Fig. 1(b). The $1Q$ domains are elevated by dozens of picometers, indicating a significant difference of DOS between $1Q$ and $3Q$ domains.

*Supported by the National Natural Science Foundation of China under Grant Nos 11574372 and 11322432, and the 'Strategic Priority Research Program (B)' of the Chinese Academy of Sciences under Grant No XDB07020300.

**Corresponding author. Email: lshan@iphy.ac.cn; xdzhu@hmfl.ac.cn

© 2017 Chinese Physical Society and IOP Publishing Ltd

More details can be seen in the enlarged topography as shown in Figs. 1(c) and 1(d), together with their respective Fourier transforms in Figs. 1(e) and 1(f). The atomic arrangements of the two phases are obviously different from that of the 2H-$NbSe_2$ phase as illustrated in Fig. 1(g). As presented in Fig. 1(h), the primary vectors determined by the Fourier transform of Fig. 1(g) reveal a CDW order with a periodicity of $3a \times 3a$, which is distinct from that of $2a_1 \times 2a_2$ ($3Q$) and $4a$ ($1Q$) as shown in Figs. 1(e) and 1(f), respectively.

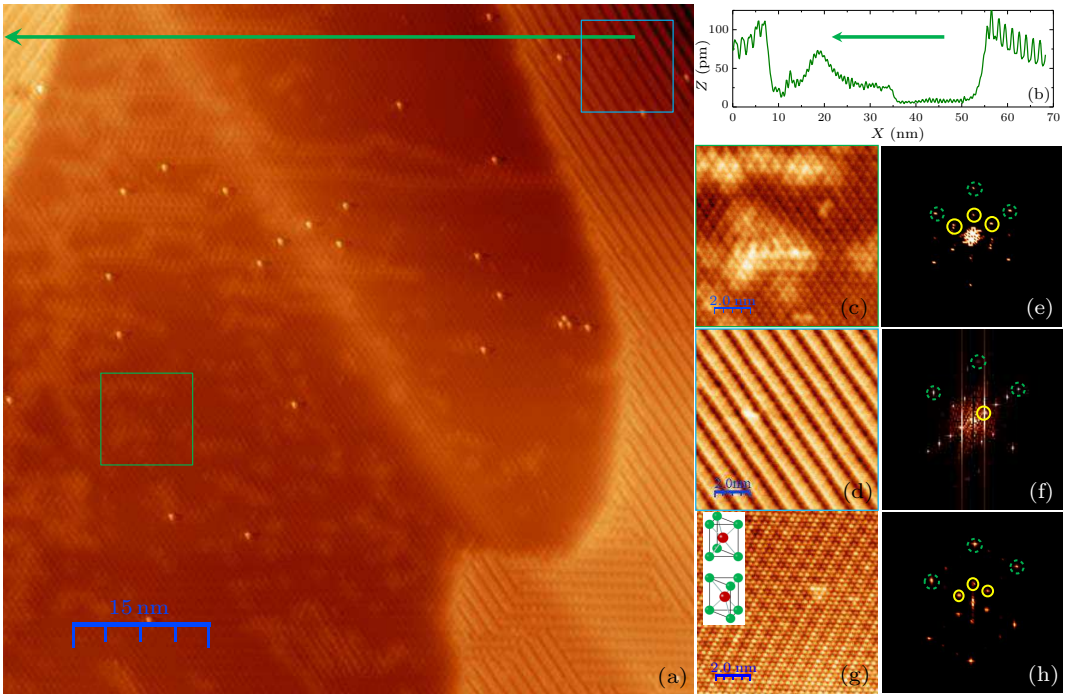

Fig. 1. (Color online) (a) Topographic image of a 75 nm square field of view, showing a reconstructed surface of a 2H-$NbSe_2$ single crystal. Setpoint parameters: bias voltage $V_b = -50$ mV and setpoint current $I_s = 35$ pA. (b) A topographic profile extracted along the arrow shown in (a), cutting through two types of superstructures. [(c), (d)] Zoomed-in atomic-resolved STM images of the triangular 2×2 and unidirectional stripe superstructures, respectively. [(e), (f)] Fourier transformations of the topographies shown in (c) and (d). The dominant CDW wavevector (yellow circle) and Bragg vector (dashed green circle) are indicated. Setpoint parameters: $V_b = -50$ mV and $I_s = 0.2$ nA. (g) A regular topographic image of 2H-$NbSe_2$, showing the typcial CDW with $3a_0$ periodicity, corresponding to a wave vector of $\frac{1}{3}q_0$ as indicated in the Fourier transformation of the image in (h). Setpoint parameters: $V_b = -20$ mV and $I_s = 0.3$ nA. Inset: the crystal structure diagrammatic sketch of 2H-$NbSe_2$, with layers of Nb (red) atoms sandwiched between layers of Se (green) atoms.

The 2×2 superstructure has been observed in 1T-$TiSe_2$, which undergoes a chiral CDW transition into a $2 \times 2 \times 2$ superlattice at about 200 K.[25–29] However, a monolayer of 1T-$NbSe_2$ fabricated by the van der Waals epitaxy technique exhibits a modulation with a periodicity of $\sqrt{13} \times \sqrt{13}$,[30] similar to the cases of bulk 1T-$TaSe_2$[16] and 1T-TaS_2.[17,20,21] The 2×2 superlattice has also been observed on the surface of high-concentration Fe-intercalated 2H-$NbSe_2$, which is attributed to the ordered Fe occupancy in the octahedral holes.[31] However, this is not consistent with our situation without any intercalation.

The $1Q$ phase is found to be continuously connected to the $3Q$ phase, maintaining the integrity of the atomic lattice and thus excluding the effect of the grain boundary. In addition, the $2a$ periodicity of the $3Q$ phase persists in the $1Q$ phase, indicating that the latter is established by a further rotational symmetry breaking of the former. For this reason, it is unsurprising to see some patches in the $3Q$ domain in Fig. 1(a), which are apt to form a stripe order. The $1Q$ modulation is much stronger than that of the $3Q$ phase or the original 3×3 CDW, which is similar to the unidirectional CDW caused by local strains on the surface of 2H-$NbSe_2$[32] though they have different wave vectors. The unidirectional charge order has been observed in another layered compound CaC_6[33] and was also attributed to local strains. Thus taking into account the undulation of the cleaved surface, we could ascribe the emergence of new superstructures on 2H-$NbSe_2$ to the local strains existing in the cleaved surface of our sample.[34]

The observed new superstructures spreading on the superconducting 2H-$NbSe_2$ phase provide an opportunity to study the interplay between various quantum states. To that end, we have measured tunneling spectra (dI/dV versus V) to obtain the local electronic DOS in the reconstructed domains. For

comparison, a typical tunneling spectrum of 2H-$NbSe_2$ is shown in Fig. 2(a). The data taken along the trajectory (illustrated in Fig. 1(a)) across the $1Q$ and $3Q$ phases are presented in Fig. 2(b). It can be seen clearly that the DOS of both $1Q$ and $3Q$ phases have very different shapes from that of the 2H one, though two main peaks appear around the similar energies of -0.5 eV and $+0.25$ eV for all phases. Moreover, the prominent spectral weight spanning from the Fermi level to 0.5 eV in the $1Q$ phase is seriously suppressed by entering the $3Q$ region, indicating a significant difference between their electronic states.

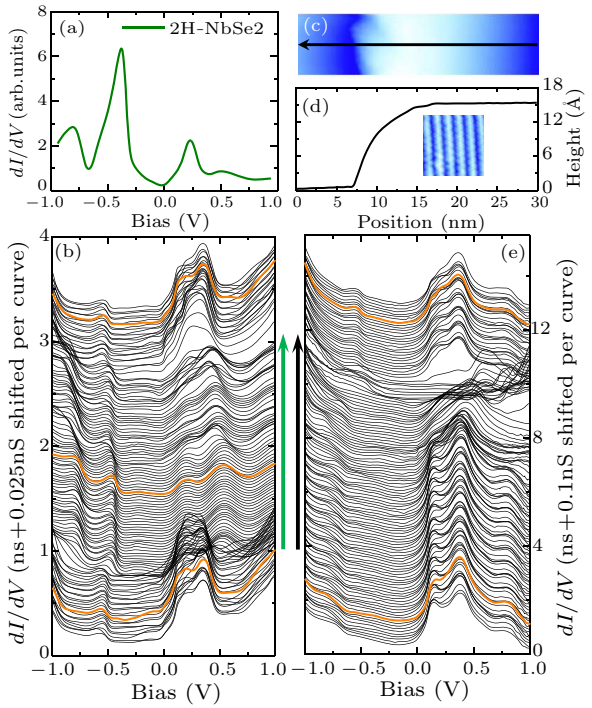

Fig. 2. (Color online) (a) Tunneling spectrum (dI/dV versus V) of 2H-$NbSe_2$. (b) Tunneling spectra taken along the arrow indicated in Fig. 1(a). Three spectra from different domains are highlighted for comparison. (c) Topography near a step. (d) Topographic profile taken along the arrow cutting through the step as indicated in (c). The step height is about 15 Å. Inset: a zoom-in image showing the details of the stripe CDW near the step. (e) Linecut of dI/dV spectra across the step taken along the arrow in (c). Two spectra taken above and below the step are highlighted for comparison.

In the field of view of the STM measurement, we observed a step with a height of about 15 Å as illustrated in Figs. 2(c) and 2(d). The height is very close to the c axis crystal parameter (12.5 Å) of 2H-$NbSe_2$, corresponding to a step of two $NbSe_2$ layers. Tunneling spectra taken in the $1Q$ domains located at both sides of the step are rather similar, separated by the exotic edge states. As shown in Fig. 2(e), the spatial resolution of 2.35 Å is precise enough to detect the DOS modulation with the same periodicity of the stripe, demonstrating a strong charge ordering in the $1Q$ phase.

To the best of our knowledge, almost all 2×2 and stripe orders observed in stoichiometric TMDs are non-superconducting, while in this work, superconductivity emerges in both $3Q$ and $1Q$ phases with an almost identical critical temperature of $T_c = 4.5$ K. To obtain further insight into the origin of such superconductivity and its interplay with the concomitant charge order, we have measured dI/dV spectra along various linecuts across domain boundaries. Some results are presented in Figs. 3(f)–3(h) corresponding to the linecuts shown in Figs. 3(a)–3(c), respectively. To check the spatial dependence of local superconductivity, we estimated superconducting gap (Δ) from the energies of coherence peaks and simultaneously calculated the conductance difference between coherence peaks and zero-bias dip (C_δ), as illustrated in Fig. 3(f). The obtained C_δ versus Δ is given in Fig. 3(k). All the points taken in various domains break into two groups, corresponding to the surfaces on two sides of the aforementioned step, respectively. The larger values of Δ and C_δ of the lower layer indicate its stronger superconductivity than that of the higher layer. As presented in Figs. 3(d) and 3(i), a detailed evolution of tunneling spectrum was measured along a linecut across the step to confirm such noticeable discrepancy. In this measurement, all data were taken from $1Q$ phases with an identical orientation to ruling out other confounding factors. The spatial dependence of both Δ and C_δ determined from Fig. 3(d) is given in Fig. 3(l), demonstrating the stronger superconductivity of the lower side than that of the higher side again.

As mentioned above, DOS varies significantly from $1Q$ to $3Q$ domains, while shows less difference across the step. On the contrary, superconductivity changes much more seriously across the step than between different domains in the same layer. In addition, although the neighboring layers above and below the step show different gap amplitudes, they have an identical critical temperature of 4.5 K, which is smaller than that of the bulk 2H-$NbSe_2$. All these facts support that the superconductivity of both $1Q$ and $3Q$ phases originates from proximity effect due to their adjacency to the underlying superconducting 2H phase.

To study the interaction between the strong charge order and superconductivity coexisting in the $1Q$ phase, spatial dependent spectra have been taken along the trajectory crossing the stripes with an interval of 1.6 Å, as indicated in Figs. 3(e) and 3(j). The determined Δ and C_δ versus position is given in Fig. 3(m), showing an obvious variation with the same periodicity of the stripes. In other words, the proximity-induced surface superconductivity can be modulated by charge ordering in an unexpected scale of 10.2 Å, which is much smaller than the coherence length ($\xi \approx 80$ Å) of the underlying bulk 2H-$NbSe_2$.[35]

This deserves to be extensively studied for the understanding of both the proximity effect and interplay between charge orders and superconductivity. Furthermore, the correlation between strain-induced charge orders and superconductivity observed here should be considered cautiously when $NbSe_2$ is used as a basement to create novel electronic states, such as topological superconductivity and Majorana bound states.[36,37] The weak van der Waals coupling between adjacent layers and the strain-sensitive surface states may significantly impact on the creation, modification, and control of such states. On the other hand, however, it provides another approach to seek and manipulate various quantum states.[38]

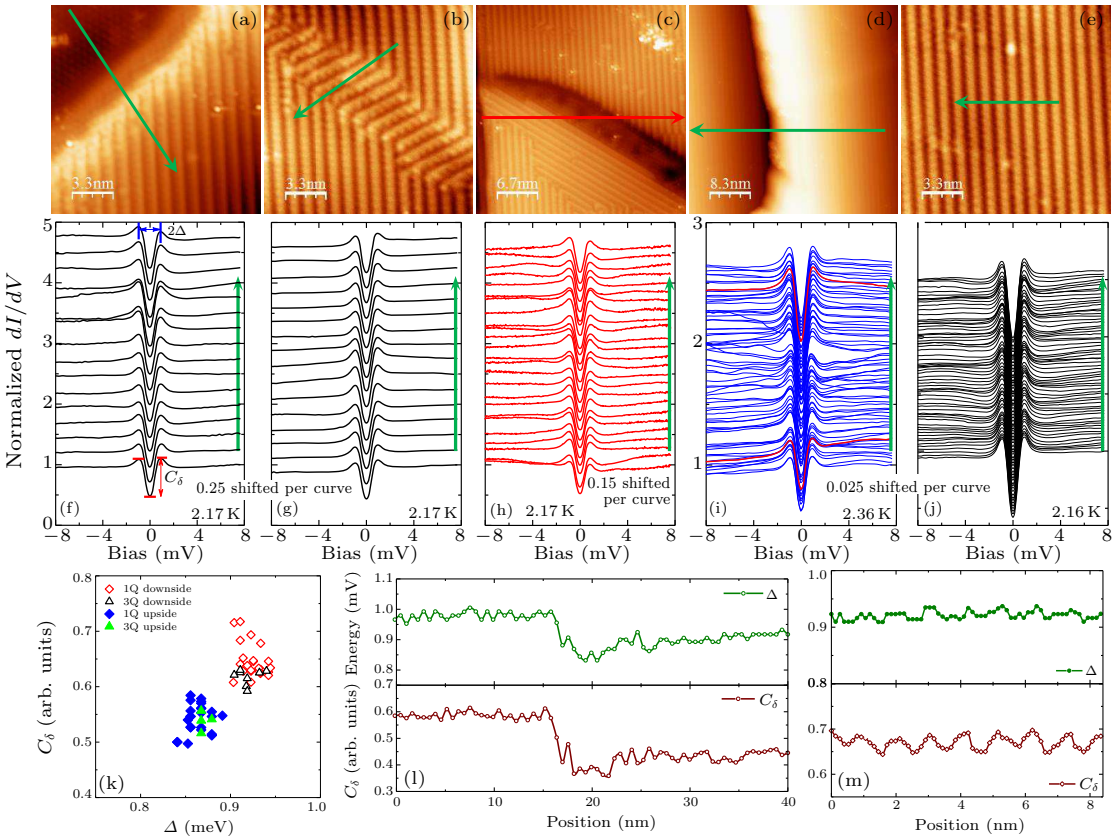

Fig. 3. (Color online) Topographic images of the reconstructed surface of $NbSe_2$ taken in various regions including (a) a 1Q–3Q interface in the layer below the step above mentioned; (b) interfaces between two 1Q phases with different orientations in the same layer in (a); (c) the 1Q–3Q interfaces in the layer above the step; (d) the step identical to that aforementioned; and (e) the pure 1Q phase. (f)–(j) Linecuts of dI/dV spectra taken along the arrows indicated in (a)–(e), respectively. (k) Statistics of Δ and C_δ determined from normalized spectra in linecut spectra of dI/dV in (f)–(h). Shapes and colors of symbols represent the type of superstructures. Solid symbols mean that the data are collected from the layer above the step, while open means below. Superconductivity is distinct on the different sides of the step. (l) Spatial dependence of gaps and C_δ along the arrows in (d). (m) Periodic modulation of gaps and C_δ obtained from the spectral linecut presented in (j).

In summary, we have observed two types of strain-induced superstructures on the cleaved surface of 2H-$NbSe_2$ single crystal. Distinct change occurs in the DOS from the triangular phase to the stripe one. On the contrary, the detected superconducting gaps are nearly homogeneous for all domains in the same layer, while very different between the layers below and above a step. In addition, the neighboring layers have an identical critical temperature much smaller than that of the bulk. We could thus conclude that the superconductivity observed on the reconstructed surface is induced by the proximity effect due to its adjacency to the underlying bulk 2H-$NbSe_2$. Modulation of superconductivity caused by the coexisting charge orders needs more theoretical considerations and may shed light on the correlation between superconductivity and CDW.

The analysis of some topographic images was made using the software WSxM.[39]

References

[1] Mazin I, Singh D, Johannes M and Du M 2008 *Phys. Rev. Lett.* **101** 057003
[2] Norman M R, Pines D and Kallin C 2005 *Adv. Phys.* **54** 715
[3] Johnston D C 2010 *Adv. Phys.* **59** 803
[4] Kivelson S A, Bindloss I P, Fradkin E, Oganesyan V, Tranquada J M, Kapitulnik A and Howald C 2003 *Rev. Mod.*

Phys. **75** 1201
[5] Wilson J A, Di Salvo F J and Mahajan S 1974 *Phys. Rev. Lett.* **32** 882
[6] Wilson J A, Di Salvo F J and Mahajan S 2001 *Adv. Phys.* **50** 1171
[7] Ali M N, Xiong J, Flynn S, Tao J, Gibson Q D, Schoop L M, Liang T, Haldolaarachchige N, Hirschberger M, Ong N P and Cava R J 2014 *Nature* **514** 205
[8] Soluyanov A A, Gresch D, Wang Z, Wu Q, Troyer M, Dai X and Bernevig B A 2015 *Nature* **527** 495
[9] Sun Y, Wu S C, Ali M N, Felser C and Yan B H 2015 *Phys. Rev.* B **92** 161107
[10] Morosan E, Zandbergen H W, Dennis B S, Bos J W G, Onose Y, Klimczuk T, Ramirez A P, Ong N P and Cava R J 2006 *Nat. Phys.* **2** 544
[11] Baugher B, Churchill H, Yang Y and Jarillo-Herrero P 2013 *Nano Lett.* **13** 4212
[12] Chhowalla M, Shin H, Eda G, Li L, Loh K and Zhang H 2013 *Nat. Chem.* **5** 263
[13] Li H, Wu J, Yin Z and Zhang H 2014 *Acc. Chem. Res.* **47** 1067
[14] Jariwala D, Sangwan V, Lauhon L, Marks T and Hersam M 2014 *ACS Nano* **8** 1102
[15] Lv R, Robinson J, Schaak R, Sun D, Sun Y, Mallouk T and Terrones M 2015*Acc. Chem. Res.* **48** 56
[16] Zhang J, Liu J, Huang J L, Kim P and Lieber C M 1996 *Science* **274** 757
[17] Kim J, Park C, Yamaguchi W, Shiino O, Kitazawa K and Hasegawa T 1997 *Phys. Rev.* B **56** R15573(R)
[18] Wang H, Lee J, Dreyer M and Barker B 2009 *J. Phys.: Condens. Matter* **21** 265005
[19] Duerloo K N, Li Y and Reed E J 2014*Nat. Commun.* **5** 4214
[20] Cho D, Cheon S, Kim K, Lee S, Cho Y, Cheong S and Yeom H 2016 *Nat. Commun.* **7** 10956
[21] Ma L, Ye C, Yu Y, Lu X, Niu X, Kim S, Feng D, Tománek D, Som Y, Chen X and Zhang Y 2016*Nat. Commun.* **7** 10453
[22] Huang H, Fan X, Singh D, Chen H, Jiang Q and Zheng W 2016 *Phys. Chem. Chem. Phys.* **18** 4086
[23] Moncton D E, Axe J D and DiSalvo F J 1975 *Phys. Rev. Lett.* **34** 734
[24] Ikebe M, Katagiri K, Noto K and Muto Y 1980 *Phys. B+C* **99** 209
[25] Ishioka J, Liu Y H, Shimatake K, Kurosawa T, Ichimura K, Toda Y, Oda Y and Tanda S 2010 *Phys. Rev. Lett.* **105** 176401
[26] Ishioka J, Fujii T, Katono K, Ichimura K, Kurosawa T, Oda M and Tanda S 2011 *Phys. Rev.* B **84** 245125
[27] Iavarone M, Di Capua R, Zhang X, Golalikhani M, Moore S and Karapetrov G 2012 *Phys. Rev.* B **85** 155103
[28] Novello A, Hildebrand B, Scarfato A, Didiot C, Monney G, Ubaldini A, Berger H, Bowler D, Aebi P and Renner C 2015 *Phys. Rev.* B **92** 081101(R)
[29] Novello A M, Spera M, Scarfato A, Ubaldini A, Giannini E, Bowler D R and Renner C 2017 *Phys. Rev. Lett.* **118** 017002
[30] Nakata Y, Sugawara K, Shimizu R, Okada Y, Han P, Hitosugi T, Ueno K, Sato T and Takahashi T 2016 *NPG Asia Mater.* **8** e321
[31] Dai Z, Xue Q, Gong Y, Slough C G and Coleman R V 1993 *Phys. Rev.* B **48** 14543
[32] Soumyanarayanan A, Yee M, He Y, van Wezel J, Rahn D, Rossnagel K, Hudson E, Norman M and Hoffman J 2013 *Proc. Natl. Acad. Sci. USA* **110** 1623
[33] Rahnejat K C, Howard C A, Shuttleworth N E, Schofield S R, Iwaya K, Hirjibehedin C F, Renner Aeppli G and Ellerby M 2011 *Nat. Commun.* **2** 558
[34] Flicker F and van Wezel J 2015 *Phys. Rev.* B **92** 201103R
[35] Hess H F, Robinson R B, Dynes R C, Valles Jr. J M and Waszczak J V 2001 *J. Vac. Sci. Technol.* B **19** 1150
[36] Xu J, Wang M, Liu Z, Ge J, Yang X, Liu C, Xu Z, Guan D, Gao C, Qian D, Liu Y, Wang Q, Zhang F, Xue Q and Jia J 2015 *Phys. Rev. Lett.* **114** 017001
[37] Sun H, Zhang K, Hu L, Li C, Wang G, Ma H, Xu Z, Gao C, Guan D, Li Y, Liu C, Qian D, Zhou Y, Fu L, Li S, Zhang F and Jia J 2016 *Phys. Rev. Lett.* **116** 257003
[38] He W, Zhou B, He J, Zhang T and Law K 2016 arXiv:1604.02867 [cond-mat.supr-con]
[39] Horcas I, Fernández R, Gómez-Rodríguez J M, Colchero J, Gómez-Herrero J and Baro A M 2007 *Rev. Sci. Instrum.* **78** 013705